JOURNAL OF CATALYSIS 130, 577–587 (1991)

Dehydrocyclization of C_6–C_8 *n*-Paraffins to Aromatics over TiO_2–ZrO_2 Catalysts

JINGLY FUNG AND IKAI WANG[1]

Department of Chemical Engineering, National Tsing Hua University, Hsinchu, Taiwan, Republic of China

Received August 24, 1990; revised January 24, 1991

This study examined the catalytic behavior of TiO_2–ZrO_2 and the mechanism of *n*-paraffins dehydrocyclization. The results showed that TiO_2–ZrO_2 calcined at 823 K gave higher aromatic selectivity and activity than other catalysts calcined at higher temperatures. The activity can be poisoned by adding small amounts of K_2O or B_2O_3 onto TiO_2–ZrO_2. The aromatization rate was correlated with the site density of the paired acid–base sites on the catalysts. The results indicated that the active centers consisted of both acid and base sites, and that only the paired acid–base sites played the primary role in the dehydrocyclization reaction. The results also showed that the apparent overall kinetics of *n*-heptane conversion was a first-order reaction. It was conclusively shown that the five-membered ring alkylcyclopentanes were not the intermediates in the transformation of *n*-paraffins into aromatics. The results showed that the *n*-paraffin was first adsorbed on the paired acid–base sites, and two hydrogen atoms were abstracted by the catalyst. Then the adsorbed molecules proceeded to cyclization through a direct six-membered ring closure without desorption, before dehydrogenation to aromatics.

INTRODUCTION

The dehydrocyclization of paraffins, first achieved in 1936 using a chromium oxide catalyst (*1*), is a critical reaction in the conversion of low octane *n*-paraffin compounds to high octane aromatic products. Numerous studies (*2–15*) have explored the dehydrocyclization mechanism. Although 1,3-ring, 1,4-ring (*2*), 1,7-ring, and 1,8-ring (*3*) in the transition state of cyclization have been found, it is widely accepted that the five- and six-membered ring closures are the primary intermediates in the cyclization reaction. Twigg (*10*) demonstrated that the mechanism of paraffin dehydrocyclization involves a two-point contact between catalysts and reactants. Furthermore, studies have shown that the reaction path follows as paraffin → olefin → cyclohexane → aromatics, when Cr_2O_3–Al_2O_3 and MoO_3–Al_2O_3 catalysts are used (*11–13*).

It has been confirmed that metal-supported monofunctional catalyst directly converts paraffins to cycloparaffins through five- and six-membered ring closures (*16, 17*). However, the metal-acid bifunctional catalyst, Pt/γ-Al_2O_3, operates according to Mills *et al.*'s mechanism (*18*). In this mechanism, the dehydrogenation occurs on the metal centers and cyclization occurs on the acid centers, with *n*-olefins and alkylcyclopentanes as the key intermediates (*19*).

Recently, studies on the selectivity of the isomerization of 1-methylcyclohexene oxide (*20*) and cyclohexene oxide (*21*) over a TiO_2–ZrO_2 catalyst illustrated the acid–base bifunctional mechanism. For the dehydrogenation of ethylbenzene and ethylcyclohexane over a TiO_2–ZrO_2 catalyst, Wang and co-workers (*22–24*) proposed a push and pull mechanism on the paired acid–base sites. However, the dehydrocyclization of paraffins over such acid–base bifunctional catalysts has never been investigated. Hence, this work attempts to correlate the catalytic properties of TiO_2–ZrO_2 with the dehydrocyclization of C_6–C_8 *n*-par-

[1] To whom correspondence should be addressed.

0021-9517/91 $3.00

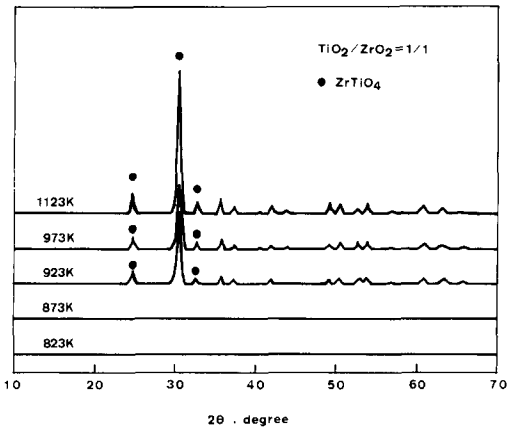

FIG. 1. X-ray diffraction pattern of TiO_2–ZrO_2 at various calcination temperatures.

affins. In addition, the reaction mechanism is also investigated.

EXPERIMENTAL

Preparation of Catalysts

An anhydrous alcohol solution containing equal moles of titanium tetrachloride and zirconium tetrachloride was added to 25% aqueous ammonia. The precipitate was aged at room temperature for 1 h, washed with deionized water until no chloride ions were detected by the addition of $AgNO_3$ to the filtrate, and then dried at 393 K for 12 h. The dried precipitate was calcined in air at various temperatures between 823 and 1123 K for 2 h at a step rate of 50 K/0.5 h.

K_2O/TiO_2–ZrO_2, which contained 0.5–2.0 wt% K_2O, was prepared from TiO_2–ZrO_2(1/1) calcined at 823 K by the incipient wetness method with potassium hydroxide. The incipient wetness method was carried out by adding the aqueous solution of KOH to the TiO_2–ZrO_2 solids. The water was then evaporated to dryness at room temperature for 48 h. This was followed by drying at 393 K for 12 h at a step rate of 1 K/min and calcining in air at 823 K for 2 h at a step rate of 50 K/0.5 h. Another sample, B_2O_3/TiO_2–ZrO_2 with 0.5–2.0 wt% of B_2O_3, was prepared from TiO_2–ZrO_2(1/1) by adding orthoboric acid (H_3BO_3) using the same methodology. The commercial catalyst, R-62 with 0.22% Pt and 0.44% Re on γ-Al_2O_3, was provided by Chinese Petroleum Corporation.

Characterization of Catalyst

X-ray diffraction patterns were measured over the range of $2\theta = 10$–$70°$ for the powder samples as shown in Fig. 1. The specific surface area of catalysts was determined by applying the BET method. The amount of acid and base sites on the catalysts was measured by applying the *n*-butylamine and acetic acid adsorption method used by Wang *et al.* (*22, 23*). These results are compiled in Table 1.

Reaction Equipment and Experimental Procedure

Catalytic reaction was carried out in a continuous flow fixed-bed microreactor. A stream of nitrogen at a designated flow rate was passed through hydrocarbon (C_6–C_8 hydrocarbons) saturators. Another nitrogen stream was used to control the partial pressure of hydrocarbon in feed. The third stream of nitrogen, air, or hydrogen was used to pretreat the catalyst. The reactor is a quartz glass tube with two layers of quartz glass separated by a layer of catalyst particles (0.5 g, 12–20 mesh). The catalyst was pretreated with air at 813 K or hydrogen at 773 K for 2 h, and then purged with nitrogen to the designated reaction temperature. The reaction was studied under the following conditions: temperature, 793–813 K; total pressure, 101.2 KPa; hydrocarbon partial pressure, 0.53–5.3 KPa; hydrogen partial pressure, 0–20.0 KPa; gas hourly space velocity (GHSV), 6,000–30,000 v/v/h.

Both feed and product were analyzed by a HP 5890A gas chromatograph (GC) equipped with a flame ionization detector (FID) and a HP 3394A data processor. The column chosen for analysis was a HP fused silica capillary column crosslinked methyl silicone with a column length of 25 m. The GC was operated under the following conditions: oven temperature, 313 K; injection temperature, 473 K; detector temperature,

TABLE 1

Acid, Base, Paired Acid–Base Amount, and Surface Area of Oxides

Oxide	Acid amount (m mole/g)	Base amount (m mole/g)	Acid–base amount[a] (m mole/g)	Surface area (m^2/g)
TiO_2–ZrO_2 (1123 K)	0.15	0.17	0.15	19.30
TiO_2–ZrO_2 (973 K)	0.40	0.38	0.38	46.02
TiO_2–ZrO_2 (923 K)	0.59	0.49	0.49	60.66
TiO_2–ZrO_2 (873 K)	0.98	0.12	0.98	136.94
TiO_2–ZrO_2 (823 K)	1.21	1.34	1.21	166.15
0.5% K_2O/TiO_2–ZrO_2	1.19	1.39	1.19	156.39
1.0% K_2O/TiO_2–ZrO_2	1.17	1.42	1.17	158.78
1.5% K_2O/TiO_2–ZrO_2	1.08	1.43	1.08	153.87
2.0% K_2O/TiO_2–ZrO_2	0.98	1.46	0.98	148.20
0.5% B_2O_3/TiO_2–ZrO_2	1.24	1.33	1.24	166.14
1.0% B_2O_3/TiO_2–ZrO_2	1.16	1.29	1.16	164.95
1.5% B_2O_3/TiO_2–ZrO_2	1.14	1.23	1.14	157.15
2.0% B_2O_3/TiO_2–ZrO_2	1.07	1.18	1.07	154.27

[a] The amount of acid or base sites, whichever is lower.

543 K; flow rate, 1 ml/min N_2; split ratio, 25; injection volume, 1 ml gas.

Data Analysis

In this study, catalyst performances are expressed according to the following formulas (*n*-heptane is used as an example):

Conversion (wt%)

$$= \frac{(n\text{-heptane})_{\text{inlet}} - (n\text{-heptane})_{\text{outlet}}}{(n\text{-heptane})_{\text{inlet}}} \times 100$$

Product selectivity, S_i (wt%)

$$= \frac{\text{product } (i)}{(n\text{-heptane})_{\text{inlet}} - (n\text{-heptane})_{\text{outlet}}} \times 100$$

Product yield, Y_i (wt%)

$$= \frac{\text{product } (i)}{(n\text{-heptane})_{\text{inlet}}} \times 100$$

RESULTS AND DISCUSSION

Comparison of γ-Al_2O_3, TiO_2–ZrO_2, and Pt–Re/γ–Al_2O_3

The results of the dehydrocyclization of *n*-heptane over γ-Al_2O_3, TiO_2–ZrO_2, and Pt–Re/γ-Al_2O_3 (R-62) catalysts are shown in Table 2. Catalysts pretreated with air (O) were under two different reaction conditions: feed flow containing hydrogen (II) and no hydrogen (I). Catalysts pretreated with hydrogen (R) were under only a feed flow containing hydrogen (II). TiO_2–ZrO_2 had higher activity and better selectivity than γ-Al_2O_3, a weak acid catalyst, which had only cracking products. In particular, aromatic selectivities of air-pretreated TiO_2–ZrO_2 were higher than those of air-pretreated Pt–Re/γ-Al_2O_3 under both reaction conditions. It is clear that the acid–base bifunctional catalyst, TiO_2–ZrO_2, can dehydrocyclize *n*-heptane with high aromatic selectivity. Figures 2 and 3 show the total conversion and aromatic yield as a function of time on stream over TiO_2–ZrO_2 and Pt–Re/γ-Al_2O_3 catalysts, respectively. As shown in Fig. 2, under a feed flow containing hydrogen, the TiO_2–ZrO_2 catalyst which was pretreated with hydrogen had the highest initial activity and aromatic yield, but deactivated gradually. Conversely, under a feed flow containing no hydrogen, the TiO_2–ZrO_2 catalyst which was pretreated with air had the lowest initial activity and aromatic yield, but the activity increased gradually. This reaction reached a stable value at 5 h on stream, and had both the highest conversion and the highest aromatic selectivity, as shown in Table 2. Figure 3

TABLE 2

Dehydrocyclization of *n*-Heptane over γ-Al_2O_3, TiO_2–ZrO_2, and R-62 Catalysts

Catalyst[a]	Reaction[b] condition	Conversion[c] (wt%)	Product selectivity (wt%)				
			$S_{C_1+C_2}$	$S_{C_3+C_4}$	$S_{C_5+C_6}$	$S_{iC_7+C_7^{2-}}$	$S_{aro.}$
γ-Al_2O_3 (O)	(I)	0.70	54	39	7	0	0
γ-Al_2O_3 (O)	(II)	0.90	54	36	10	0	0
γ-Al_2O_3 (R)	(II)	0.96	53	35	12	0	0
TiO_2–ZrO_2(O)	(I)	8.34	6	7	1	16	70
TiO_2–ZrO_2(O)	(II)	7.13	19	9	8	7	57
TiO_2–ZrO_2(R)	(II)	7.37	16	9	9	14	52
R-62 (O)	(I)	6.52	9	17	6	16	52
R-62 (O)	(II)	13.76	15	35	14	19	17
R-62 (R)	(II)	54.79	11	15	6	4	64

[a] (O): Catalysts were pretreated with air at 813 K for 2 h; (R): catalysts were pretreated with hydrogen at 773 K for 2 h.

[b] (I): P_{nC_7} = 1.6 KPa, P_{N_2} = 99.6 KPa, T = 793 K, GHSV = 6000; (II): P_{nC_7} = 1.6 KPa, P_{H_2} = 20.0 KPa, P_{N_2} = 79.6 KPa, T = 793 K, GHSV = 6000.

[c] Time on stream: 5 h.

shows that the hydrogen-pretreated Pt–Re/γ-Al_2O_3 catalyst possessed the highest activity but deactivated quickly. The air-pretreated Pt–Re/γ-Al_2O_3 catalyst gave better stability but lower activity.

Correlation of Acid and Base Properties of TiO_2–ZrO_2 with Their Catalytic Performance

Wang *et al.* (*22*) and Wu *et al.* (*24*) proved that the formation of $ZrTiO_4$ crystals as well as the amount of acid and base sites on TiO_2–ZrO_2 catalysts were the major factors affecting the catalytic activity on the dehydrogenation of ethylbenzene. Since TiO_2–ZrO_2 showed good aromatic selectivity of the dehydrocyclization of *n*-heptane, it is worthwhile to investigate whether $ZrTiO_4$ crystals or the amount of acid and base sites on the catalysts plays the primary role in this reaction.

Figure 4 shows the total conversion and product yield of the dehydrocyclization of *n*-heptane over TiO_2–ZrO_2 calcined between 823 and 1123 K. The total conversion and aromatic yield decreased with increasing calcination temperature. The yield of dehydrogenation and isomerization products reached a maximum value when TiO_2–ZrO_2 was calcined at 923 K. This could be explained by the formation of $ZrTiO_4$ crystals, as shown in Fig. 1, which were also the active centers of the dehydrogenation of ethylbenzene (*24*). However, the formation of $ZrTiO_4$ crystals did not increase aromatization activity. This demonstrates that $ZrTiO_4$ crystals are not the active centers of the aromatization reaction. As shown in Table 1, the amount of acid and base sites decreased with increasing calcination temperature. By comparing the aromatic yield with the amount of acid and base sites, it was found that the aromatic yield increased as the amount of acid and base sites increased. This shows that the amount of acid and base sites on TiO_2–ZrO_2 is the factor affecting the aromatization reaction.

In addition, doping with a small amount of K_2O and B_2O_3 decreased the amount of acid and base sites, respectively, as shown in Table 1. Figures 5 and 6 show that increasing both the K_2O and B_2O_3 content reduced the total conversion of *n*-heptane. This was due to the decreased acidity or basicity of

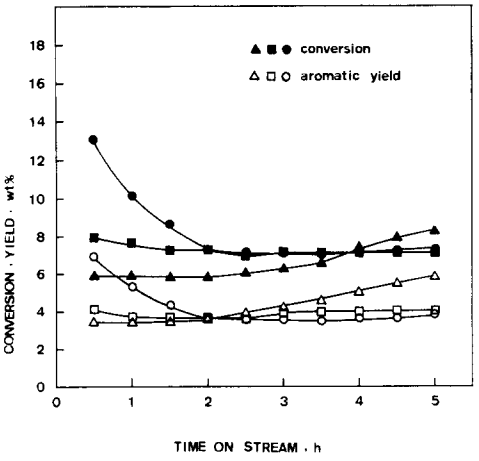

FIG. 2. Total conversion and aromatic yield as a function of time on stream over TiO_2–ZrO_2 catalysts. (▲, △), catalysts pretreatment and reaction conditions as in Table 2 (O), (I); (■, □), catalysts pretreatment and reaction conditions as in Table 2 (O), (II); (●, ○), catalysts pretreatment and reaction conditions as in Table 2 (R), (II).

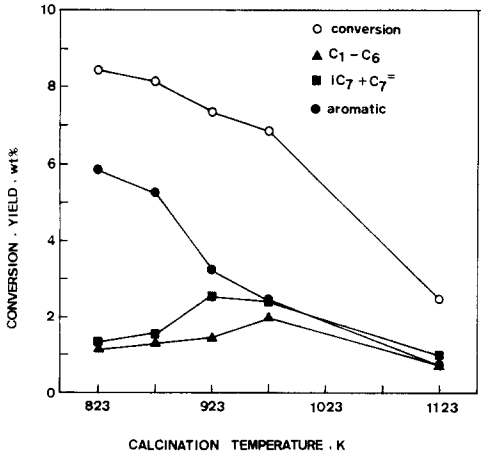

FIG. 4. Total conversion and the yield of products over TiO_2–ZrO_2 at various calcination temperatures. Reaction conditions: P_{nC_7} = 1.6 KPa, P_{N_2} = 99.6 KPa, T = 793 K, GHSV = 6000.

TiO_2–ZrO_2 which was poisoned by K_2O and B_2O_3. Adding 0.5% K_2O on TiO_2–ZrO_2 yielded maximum aromatic selectivity and reduced the isomerization and dehydrogenation products. However, the aromatic yield sharply decreased with further increase in K_2O content, while the other reactions did not have any significant change. Doping B_2O_3 showed trends similar to doping K_2O. The higher aromatic selectivity over 0.5% K_2O/TiO_2–ZrO_2 and 0.5% B_2O_3/TiO_2–ZrO_2 could be explained by the poisoning of some strong acid and base sites by

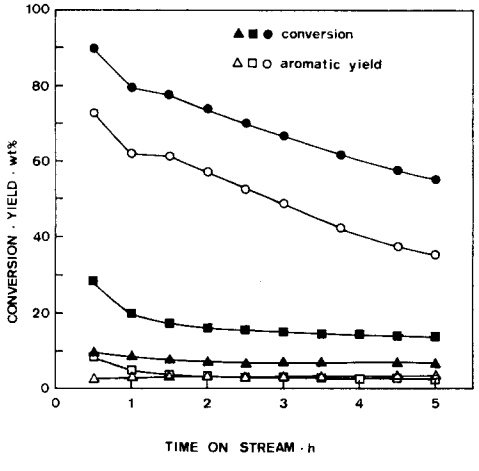

FIG. 3. Total conversion and aromatic yield as a function of time on stream over Pt–Re/γ-Al_2O_3 catalysts. All symbols as in Fig. 2.

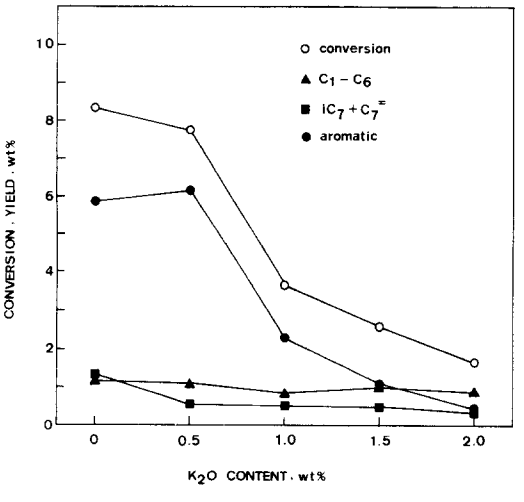

FIG. 5. Effect of doping with K_2O on the total conversion and the yield of products. Reaction conditions: P_{nC_7} = 1.6 KPa, P_{N_2} = 99.6 KPa, T = 793 K, GHSV = 6000.

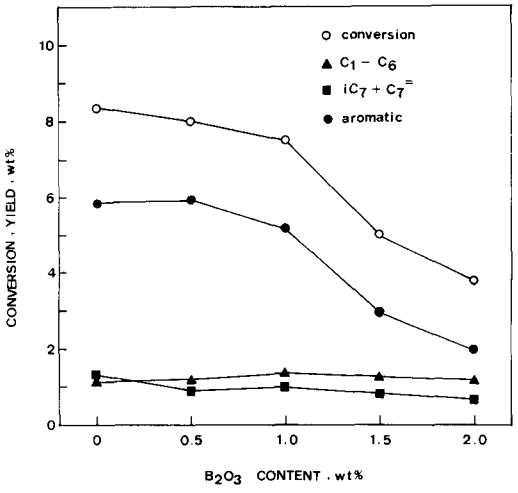

FIG. 6. Effect of doping with B_2O_3 on the total conversion and the yield of products. Reaction conditions: P_{nC_7} = 1.6 KPa, P_{N_2} = 99.6 KPa, T = 793 K, GHSV = 6000.

K_2O and B_2O_3. The acid and base sites with moderate strength could be used together to cyclize the *n*-heptane and facilitate the aromatization reaction.

The above results of K_2O/TiO_2–ZrO_2 and B_2O_3/TiO_2–ZrO_2 catalysts provide further evidence that both acid and base sites play the primary roles in the dehydrocyclization of *n*-heptane. However, it seems that neither the acid site nor the base site alone is the active center of the aromatization reaction. The correlation between the aromatization rate and the site density of the paired acid–base sites on the catalysts is shown in Fig. 7. It is easily shown that the aromatization rate increased linearly with the site density of the paired acid–base sites. Apparently, the activity of *n*-heptane dehydrocyclization over TiO_2–ZrO_2 catalysts was dependent upon the amount of paired acid–base sites on the catalysts. Both acid and base sites alone are active centers for the conversion of *n*-heptane, but only the paired acid–base sites can accelerate the aromatization reaction.

Concentration and Space Velocity Effects

By varying the initial concentration of reactant in feed and measuring the fractional conversion, we could determine the reaction order. Figure 8 shows the total conversion and the selectivity of products over TiO_2–ZrO_2 at various partial pressures of *n*-heptane ranging from 0.53 to 5.3 KPa. The fractional conversion was independent of the feed concentration of *n*-heptane. This indicates that the apparent overall reaction kinetics was first order. However, the product distribution changed with the feed concentration. The aromatic selectivity decreased with increasing *n*-heptane concentration. The cracking products, as well as isomerization and dehydrogenation products, increased with increasing *n*-heptane concentration. The above observations indicate that increasing the *n*-heptane concentration decreases the probability of adsorption of one *n*-heptane molecule on a paired acid–base site and thus decreases the selectivity of aromatic products. In other reactions, cracking and isomerization could proceed on one acid site or on a site which is independent of the aromatization reaction.

Now, we can analyze whether the olefins

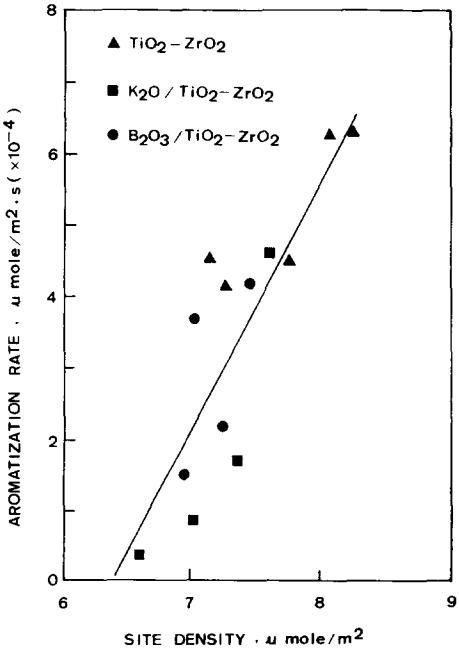

FIG. 7. Correlation between the aromatization rate and the site density of the paired acid–base sites.

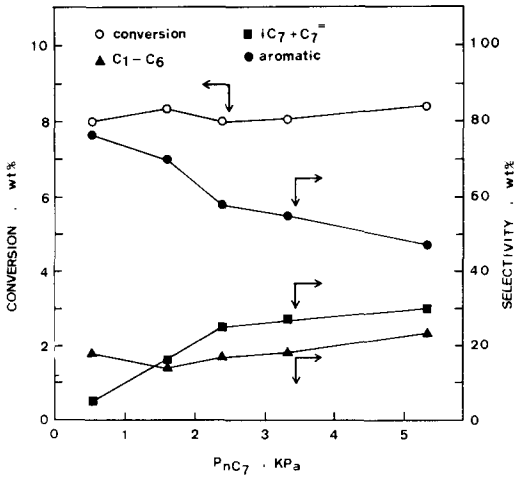

FIG. 8. Total conversion and the selectivity of products over TiO_2–ZrO_2 at various partial pressure of *n*-heptane. Reaction conditions: P = 101.2 KPa, T = 793 K, GHSV = 6000.

found in the products are intermediates or byproducts from a parallel side reaction. To investigate this question, experiments with varying contact time were carried out. As shown in Fig. 9, all the products formed increased with increasing contact time. If the olefins are the intermediates in the dehydrocyclization reaction, then the initial rate of olefins formation should be higher than other products, and the olefins yield should reach a maximum value and then decrease. However, in the operating range of this study, the amount of olefins formed increased steadily with increasing contact time. Thus, it is clear that the olefins in the products are not intermediates in the dehydrocyclization reaction but are formed by a parallel side reaction.

Postulated Mechanism of n-*Paraffin Dehydrocyclization*

Table 3 shows the conversion and product selectivity of *n*-hexane, 1-hexene, *n*-heptane, *n*-octane, and 1-octene. The reactivity of the *n*-paraffin increased with increasing the number of carbon atoms. As the *n*-paraffin length increased, the aromatization and cracking selectivities also increased, but the isomerization and dehydrogenation selectivities decreased. Those observations are similar to the results of Pt/Al_2O_3 reported in the literature (*25*).

Table 3 also showed that both *n*-hexane and *n*-octane gave significantly higher aromatic selectivity than 1-hexene and 1-octene at comparable conversion levels. If one assumes that the adsorbed *n*-paraffin dehydrogenates to olefin, which desorbs and readsorbs on another catalytic active center for cyclization, then the gas phase olefin must be an intermediate in the aromatization of *n*-paraffin. However, in this study the olefin had a lower aromatic selectivity than the *n*-paraffin over TiO_2–ZrO_2 at the same conversion level. This indicates that the adsorbed *n*-paraffin undergoes dehydrogenation with-

TABLE 3

Dehydrocyclization of *n*-Hexane, 1-Hexene, *n*-Heptane, *n*-Octane, and 1-Octene over TiO_2–ZrO_2 Catalysts[a]

Reactant	GHSV (v/v/h)	Conversion (wt%)	Product selectivity (wt%)[b]		
			$S_{cra.}$	$S_{iso.+dehy.}$	$S_{aro.}$
n-Hexane	12000	5.05	16	41	43
1-Hexene	30000	5.13	27	57	16
n-Heptane	12000	7.91	27	28	45
n-Octane	12000	10.81	29	23	48
1-Octene	30000	10.62	27	47	26

[a] Reaction conditions: P_{HC} = 2.4 KPa, P_{N_2} = 98.8 KPa, T = 813 K.

[b] Abbreviations: cra., cracking products; iso.+dehy., isomerization and dehydrogenation products; aro., aromatic products.

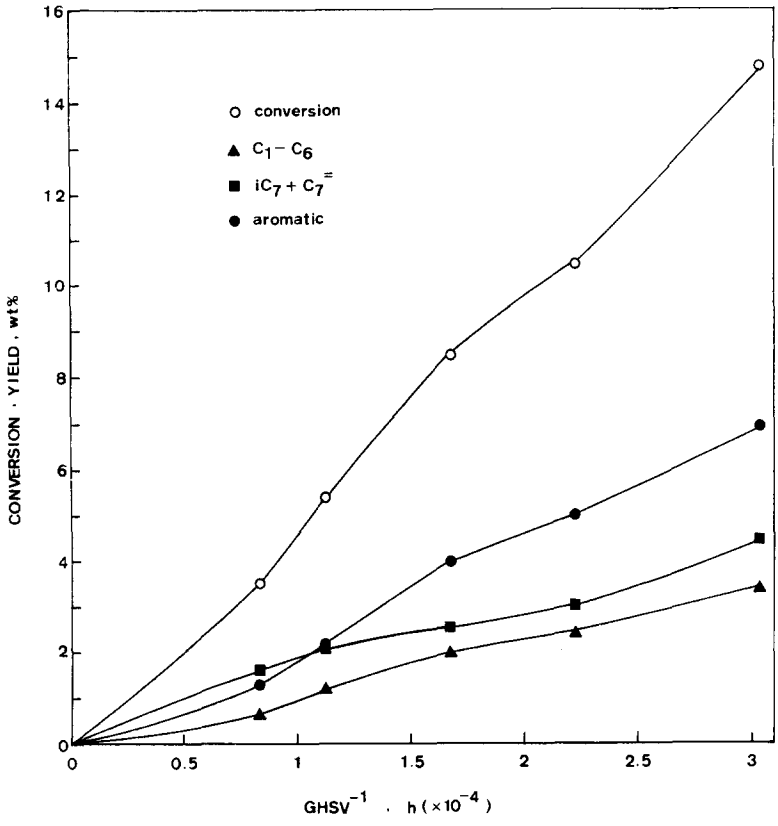

FIG. 9. Total conversion and the yield of products as a function of space velocity over TiO_2–ZrO_2. Reaction conditions: P_{nC_7} = 1.6 KPa, P_{N_2} = 99.6 KPa, T = 793 K.

out desorption and directly cyclizes on the same catalytic sites. This demonstrates that the gas phase olefin is not an intermediate in the aromatization reaction over TiO_2–ZrO_2.

Table 4 shows the conversion and the product yield of the reforming of C_6 hydrocarbons over TiO_2–ZrO_2 and R-62 catalysts. 1-Hexene gave a conversion higher than that of *n*-hexane over TiO_2–ZrO_2, but the benzene yields were approximately equal. This indicates that when *n*-hexane and 1-hexene are dehydrocyclized to benzene, they have the same adsorption rate on the paired acid–base sites. However, the more reactive 1-hexene, which can also be adsorbed on other sites, proceeds to the isomerization and cracking reactions, so that a higher conversion and a lower aromatic selectivity are observed. Table 4 also shows that the benzene yield from several C_6 hydrocarbons decreases in order of cyclohexene ≫ cyclohexane > 1-hexene ≃ *n*-hexane ≫ methylcyclopentane.

The general mechanism of *n*-hexane dehydrocyclization over commercial catalysts containing both metal and acid functions was demonstrated by Mills *et al.* (*18*). The reactions to benzene proceed through olefin intermediates with the isomerization of methylcyclopentane to cyclohexene. As shown in Table 4, methylcyclopentane was reformed over R-62 and TiO_2–ZrO_2. Reduced R-62 catalyst and air-pretreated R-62 catalyst gave 20 and 12% aromatic selectivity respectively, but the TiO_2–ZrO_2 catalyst gave no aromatics. This indicates that the dehydrocyclization of *n*-hexane to benzene over TiO_2–ZrO_2 does not proceed through

TABLE 4

Reforming of C_6 Hydrocarbons over TiO_2–ZrO_2 and R-62 Catalysts[a]

Reactant[b]	Catalyst[c]	Conversion (wt%)	Product distribution (wt%)			$S_{aro.}$ (wt%)
			$Y_{C_1-C_5}$	$Y_{iC_6+C_6^{2-}}$	$Y_{aro.}$	
n-Hexane	TiO_2–ZrO_2(O)	5.05	0.80	2.08	2.17	43
1-Hexene	TiO_2–ZrO_2(O)	16.34	4.90	9.15	2.29	14
Cyclohexane	TiO_2–ZrO_2(O)	6.90	0.13	0.89	5.88	85
Cyclohexene	TiO_2–ZrO_2(O)	68.12	2.72	4.09	61.31	90
MCP	TiO_2–ZrO_2(O)	4.63	0.37	4.26	0	0
MCP	R-62(O)	7.37	0.67	5.80	0.90	12
MCP	R-62(R)	9.27[d]	1.40	6.00	1.87	20

[a] Reaction conditions: P_{HC} = 2.4 KPa, P_{N_2} = 98.8 KPa, T = 813 K, GHSV = 12000.
[b] MCP: methylcyclopentane.
[c] (O), (R) as in Table 2.
[d] P_{HC} = 2.4 KPa, P_{H_2} = 10.0 KPa, P_{N_2} = 88.8 KPa.

the methylcyclopentane intermediate. These results strongly suggest that the reaction path of dehydrocyclization over an acid–base bifunctional catalyst, TiO_2–ZrO_2, differs from that over a metal-acid bifunctional catalyst, R-62.

According to these results in the study, we postulate the reaction path of dehydrocyclization over an acid–base bifunctional catalyst, as shown in Fig. 10. Initially, the *n*-hexane is adsorbed on the paired acid–base sites on the catalyst surface through 1-2 and 1-6 adsorption. Then, the dehydrocyclization of *n*-hexane to benzene can occur by two possible reaction routes. In route (A), the adsorbed *n*-hexane first dehydrogenates to 1-hexene without desorption, and then directly proceeds to the cyclization step on the same catalytic centers. While in route (B), the adsorbed *n*-hexane releases two hydrogen atoms while simultaneously cyclizing to the adsorbed cyclohexane, and then proceeds to the dehydrogenation step. This study cannot conclusively determine which is the primary reaction route. However, the similar benzene yields from *n*-hexane and 1-

TABLE 5

Product Distribution of Aromatic Fraction from the Dehydrocyclization of *n*-Octane over TiO_2–ZrO_2 and R-62 Catalysts[a]

Catalyst[b]	$Y_{aro.}$ (wt%)	Product distribution[d] (wt%)				
		B	T	EB+ST	O	MP
TiO_2–ZrO_2(O)	5.22	6	4	50	36	4
R-62(O)	4.52	8	13	33	8	38
R-62(R)	6.45[c]	7	9	33	4	46

[a] Reaction conditions: P_{nC_8} = 2.4 KPa, P_{N_2} = 98.8 KPa, T = 813 K, GHSV = 12000.
[b] (R), (O) as in Table 2.
[c] P_{nC_8} = 2.4 KPa, P_{H_2} = 10.0 KPa, P_{N_2} = 88.8 KPa.
[d] Abbreviations: B, benzene; T, toluene; EB + ST, ethylbenzene and styrene; O, *o*-xylene; MP, *m*-xylene, and *p*-xylene.

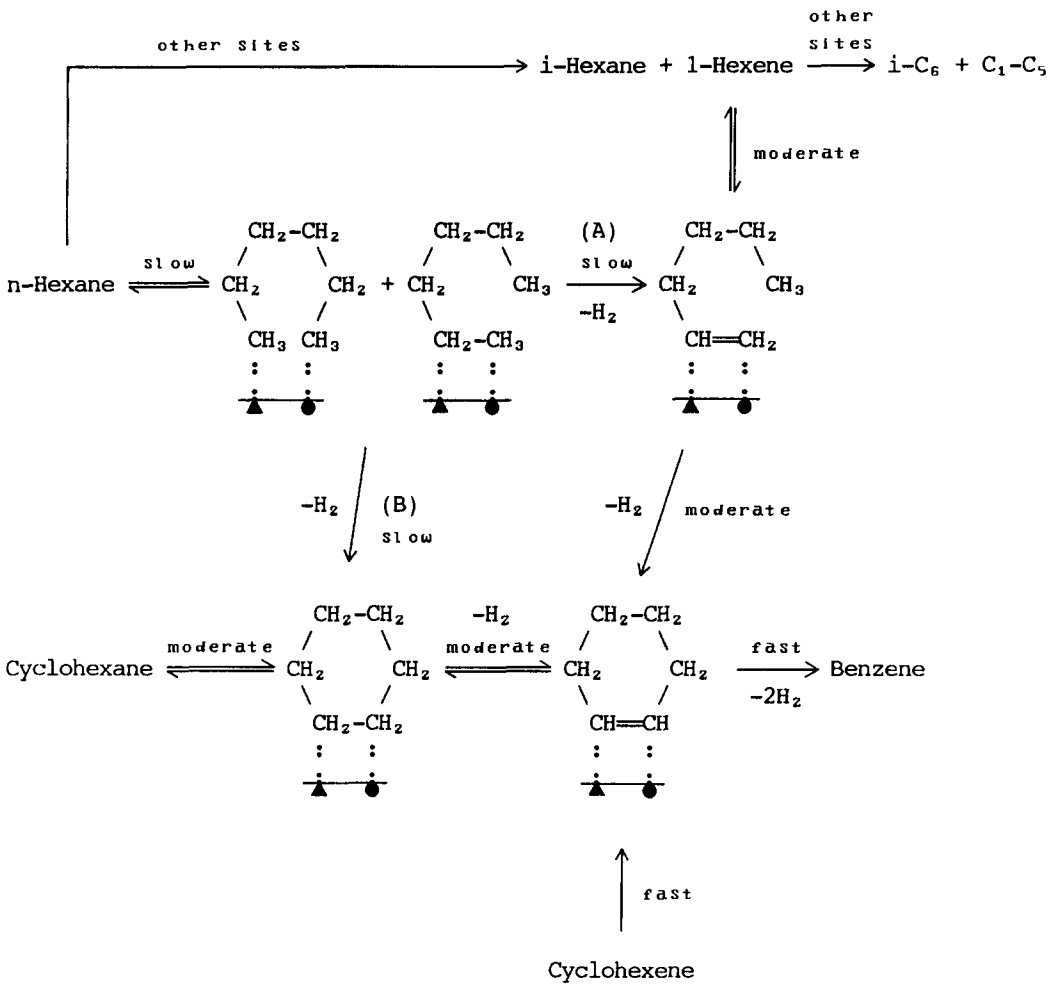

FIG. 10. The mechanism of dehydrocyclization over an acid–base catalyst. (▲) and (●) represent the acid and base sites on the catalyst surface respectively.

hexene, as shown in Table 4, suggest that the routes are parallel reactions. Overall, two major points are revealed. The first point is that the aromatization reaction proceeds on the paired acid–base sites on the catalyst surface. The second point is that the cyclization step proceeds through a direct six-membered ring closure.

Table 5 shows the product distribution of the aromatic fraction from the dehydrocyclization of *n*-octane over TiO_2–ZrO_2 and R-62 catalysts. Approximately 50% of the C_8 aromatic products over R-62 were *m*-xylene and *p*-xylene. However, more than 90% of the C_8 aromatic products over TiO_2–ZrO_2 were ethylbenzene, styrene, and *o*-xylene, while the other two C_8 isomers, *m*-xylene and *p*-xylene, were present only in small amount. According to proposals by Twigg (*10*) and Davis and Venuto (*16*), possible C_8 aromatic products predicted by a direct six-membered ring closure with *n*-octane are ethylbenzene, styrene, and *o*-xylene, as shown in Fig. 11. The formation of *m*-xylene and *p*-xylene must go through isomerization reaction or five-membered ring intermediates. It is clear that the cyclization of *n*-octane over TiO_2–ZrO_2 proceeds predomi-

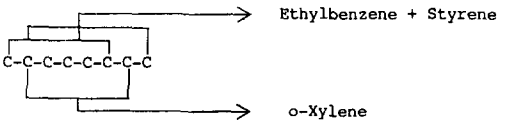

FIG. 11. Possible closures to direct six-membered ring with *n*-octane.

nantly through a direct six-membered ring closure. Over R-62, however, both five- and six-membered ring closures occur as parallel reactions, but the five-membered ring closure occurs most frequently.

The results of the dehydrocyclization of *n*-octane provide strong evidence of direct six-membered ring formation over TiO_2–ZrO_2. This corresponds to the postulated mechanism as shown in Fig. 10. That is, *n*-paraffins will be adsorbed on the paired acid–base sites and the adsorbed molecules, which release two hydrogen atoms, will cyclize to six-membered ring intermediates and then proceed through dehydrogenation to aromatics.

CONCLUSION

From the above discussion we conclude that TiO_2–ZrO_2 showed high aromatic selectivity for the dehydrocyclization of *n*-paraffins because of their acid–base properties. The adjacent acid and base sites with moderate strength were used together to facilitate the aromatization reaction. This study also postulates that the reaction path of dehydrocyclization of *n*-paraffin over an acid–base bifunctional catalyst proceeds through a direct six-membered ring closure, not through a five-membered ring closure.

ACKNOWLEDGMENTS

The authors express their gratitude for the support of this work by the Refining and Manufacturing Research Center of the Chinese Petroleum Corporation.

REFERENCES

1. Moldavski, B. L., and Kamusher, G. D., *Dokl. Akad. Nauk SSSR* **1,** 343 (1936).
2. Pines, H., and Csicsery, S. M., *J. Catal.* **1,** 313 (1962).
3. Pines, H., Goetschel, C. T., and Csicsery, S. M., *J. Org. Chem.*, 2713 (1963).
4. Steine, H., *in* "Catalysis" (P. H. Emmett, Ed.), Vol. 4, p. 529. Reinhold, New York, 1956.
5. Hansch, C., *Chem. Rev.* **53,** 353 (1953).
6. Sharan, K. M., *Catal. Rev. Sci. Eng.* **26**(2), 141 (1984).
7. Clarke, J. K. A., *Chem. Rev.* **75**(3), 291 (1975).
8. Finlayson, O. E., and Clarke, J. K. A., *J. Chem. Soc., Faraday Trans. 1* **80,** 191 (1984).
9. Sivasanker, S., and Padalkar, S. R., *Appl. Catal.* **39,** 123 (1988).
10. Twigg, G. H., *Trans. Faraday Soc.* **35,** 1006 (1939).
11. Pitkethly, R. C., and Steins, H., *Trans. Faraday Soc.* **35,** 979 (1939).
12. Hoog, H., Verheus, J., and Zuiderweg, F. J., *Trans. Faraday Soc.* **35,** 993 (1939).
13. Fogelberg, L. G., Gore, R., and Ranby, B., *Acta. Chem. Scand.* **21,** 2041 (1967).
14. Emmett, P. H., and Sabatier, P., *in* "Catalysis Then and Now" (P. H. Emmett, Ed.), Chap. 7, p. 104, 1965.
15. Paal, Z., *in* "Advances in Catalysis" (D. D. Eley, H. Pines, and P. B. Weisz, Eds.), Vol. 29, p. 273. Academic Press, New York, 1980.
16. Davis, B. H., and Venuto, P. B., *J. Catal.* **15,** 363 (1969).
17. Dautzenberg, F. M., and Platteeuw, J. C., *J. Catal.* **19,** 41 (1970).
18. Mills, G. A., Heinemann, H., Milliker, T. H., and Oblad, A. G., *Ind. Eng. Chem.* **45,** 134 (1953).
19. Parera, J. M., Beltramini, J. N., Querini, C. A., Martinelli, E. E., Churin, E. J., Aloe, P. E., and Figoli, N. S., *J. Catal.* **99,** 39 (1986).
20. Arata, K., Akutagawa, S., and Tanabe, K., *Bull. Chem. Soc. Jpn.* **49**(2), 390 (1976).
21. Arata, K., and Tanabe, K., *Bull. Chem. Soc. Jpn.* **53,** 299 (1980).
22. Wang, I., Chang, W. F., Shiau, R. J., Wu, J. C., and Chung, C. S., *J. Catal.* **83,** 428 (1983).
23. Wang, I., Wu, J. C., and Chung, C. S., *Appl. Catal.* **16,** 89 (1985).
24. Wu, J. C., Chung, C. S., Ay, C. L., and Wang, I., *J. Catal.* **87,** 98 (1984).
25. Parera, J. M., Querini, C. A., Beltramini, J. N., and Figoli, N. S., *Appl. Catal.* **32,** 117 (1987).